IVYSPRING INTERNATIONAL PUBLISHER

Theranostics

2018; 8(14): 3891-3901. doi: 10.7150/thno.24056

Research Paper

Tumor-suppressing miR-141 gene complex-loaded tissue-adhesive glue for the locoregional treatment of hepatocellular carcinoma

Min-Kyoung Kim[1,*], Young-Ah Moon[2,*], Chung Kil Song[1], Rengarajan Baskaran[1], Sijeong Bae[2], Su-Geun Yang[1,✉]

1. World Class Smart Lab, Department of New Drug Development, Inha University College of Medicine, Incheon, Republic of Korea
2. Department of Molecular Medicine, Inha University College of Medicine, Incheon, Republic of Korea

*The authors equally contributed to this work.

✉ Corresponding author: World Class Smart Lab, Department of New Drug Development, Inha University College of Medicine, 366, Seohae-daero, Jung-gu, Incheon 22332, Republic of Korea. E-mail: Sugeun.Yang@Inha.ac.kr; Tel.: +82 32 8902382; Fax: +82 32 8901199

Received: 2017.11.28; Accepted: 2018.05.18; Published: 2018.06.24

Abstract

microRNAs (miRNAs) regulate gene expression post-transcriptionally and have been extensively tested as therapeutic molecules against several human diseases. *In vivo* delivery of miRNAs needs to satisfy the following conditions: safety, efficiency, and long-term therapeutic effectiveness. To satisfy these conditions, we developed a tissue-adhesive nucleotide-polymer complex (NPX-glue) for *in vivo* delivery of miRNAs to treat hepatocellular carcinoma (HCC).

Methods: Polyallylamine (PAA), a cationic polymer, was mixed with tumor-suppressing miR-141 to form NPX and then mixed with partially oxidized alginate (OA) to form NPX-glue. Delivery efficiency of miR-141:NPX-glue was determined in cultured HCC cells and in an implanted HCC tumor model. *In vivo* tumor-suppressive effects of miR-141 on HCC were examined in mice upon intratumoral injection of miR-141:NPX-glue.

Result: NPX-glue was generated by mixing of NPX with OA, which eliminated the inherent cytotoxic effect of NPX. NPX-glue led to the efficient delivery of miR-141 and plasmid to cultured cells and solid tumors in mice, where their expression was maintained for up to 30 days. Upon intratumoral injection of miR-141:NPX-glue, the growth of the tumors was dramatically retarded in comparison with the negative control, NCmiR:NPX-glue, ($p < 0.05$). Molecular examination proved miR-141:NPX-glue efficiently regulated the target genes including *MAP4K4*, *TM4SF1*, *KEAP1*, *HDGF*, and *TIAM1* and finally induced apoptosis of cancer tissues.

Conclusion: Here, we show that NPX-glue delivers therapeutic miR-141 to solid tumors in a safe, stable, and long-term manner and prove that locoregional treatment of HCC is possible using the NPX-glue system.

Key words: miR-141, nucleotide complex, tissue adhesive glue, hepatic cancer, gene delivery

Introduction

Hepatocellular carcinoma (HCC) is the second most common cause of cancer death worldwide [1]. Surgical resection and systemic chemotherapies have been the standard procedures for cancer treatments [2, 3]. However, restricted surgical indications and toxicities from the systemic chemotherapies have brought attention to locoregional procedures, especially for unresectable or multinodular cancers [2, 3]. Recent advances in cancer imaging technologies have enabled precise access to cancers so that high-dose therapeutic modalities can be administered directly to target cancers with little undesirable systemic toxicities and maximum drug effects [4-6]. HCC is one of the cancers that can be accessed percutaneously. Locoregional approaches for HCC treatment such as chemoembolization, radioembolization, and ablation techniques have long been practiced and their beneficial effects on patients'

survival have been presented in various clinical trials [4-9]. Currently, locoregional approaches are applied to other cancers including pancreatic, prostate, and breast cancers [10-12].

HCC patients are managed based on their cancer stage [7, 8]. Locoregional therapies are mainly performed in early to intermediate-stage multinodular HCCs, which are not suitable for surgical resection [6]. Approximately 30–40% of HCC patients are eligible for locoregional treatments currently [1]. Among these treatments, therapeutics are injected or delivered to lesions in the liver via a fine needle inserted percutaneously or via a transarterial catheter [3, 13]. Multiple percutaneous injections are also possible depending on the size of the tumors [13]. To obtain the best results, efficient anti-cancer agents and well-designed delivery systems are essential [6, 14].

microRNAs (miRNAs) are small non-coding RNAs that are involved in the post-transcriptional regulation of genes. miRNA binds to the 3′ untranslated regions (UTRs) of the target genes, resulting in the degradation of mRNA and the repression of protein translation [15]. Certain miRNAs, including miR-141, are involved in the regulation of cell proliferation, differentiation, and apoptosis, and thus, could be good therapeutic agents for cancer treatment [16, 17]. The expression of miR-141 is significantly reduced in various malignant tumors, such as renal cell carcinoma [18], breast cancer [19], pancreatic cancer [20], gastric cancer [21], and HCC [22, 23]. The role of miR-141 as a tumor suppressor gene was presented in a gastric cancer model [21]. These results suggest that miR-141 may play a role as a tumor suppressor in HCC as well and could be a good candidate for the locoregional treatment of this disease when complexed with a good delivery system.

Oxidation of polysaccharides converts their alcohol groups into aldehydes, allowing various biomedical applications. Specifically, the aldehydes actively form Schiff bases with tissue proteins and act as a tissue glue in the body [24, 25]. Thus, oxidized polysaccharides can stick to the target tissue quickly and stably. Oxidized alginate (OA) has been tried as a safe and efficient surgical seal replacement [26]. Alginate-based biomaterials have been used as a scaffolding matrix to integrate different kinds of bioactive molecules and have also been suggested as an attractive delivery vehicle for the transfer of nucleic acids [26-29]. Various kinds of cationic polymers including polyallylamine (PAA) have been used as a delivery vehicle for nucleic acids (plasmid DNA and miRNAs) and can be cross-linked with OA to form a hydrogel [30-34]. PAA could be useful for *in vivo* gene delivery as it has a high density of amine groups, shows good water solubility and its cross-linked form is lower in toxicity [34].

In this study, we designed a Schiff base-forming tumor-adhesive hydrogel system for locoregional gene delivery to tumors (Scheme 1). Tumor-suppressing miR-141 was mixed with cationic PAA to generate a nucleotide-polymer complex (NPX), which was introduced into a Schiff-forming OA hydrogel (miR-141:NPX-glue). The chemical and biological properties of the NPX-glue were examined. Tumor-suppressive effects of miR-141:NPX-glue were confirmed in a human HCC-xenograft mouse model by injecting the miR-141:NPX-glue directly into the tumor lesions.

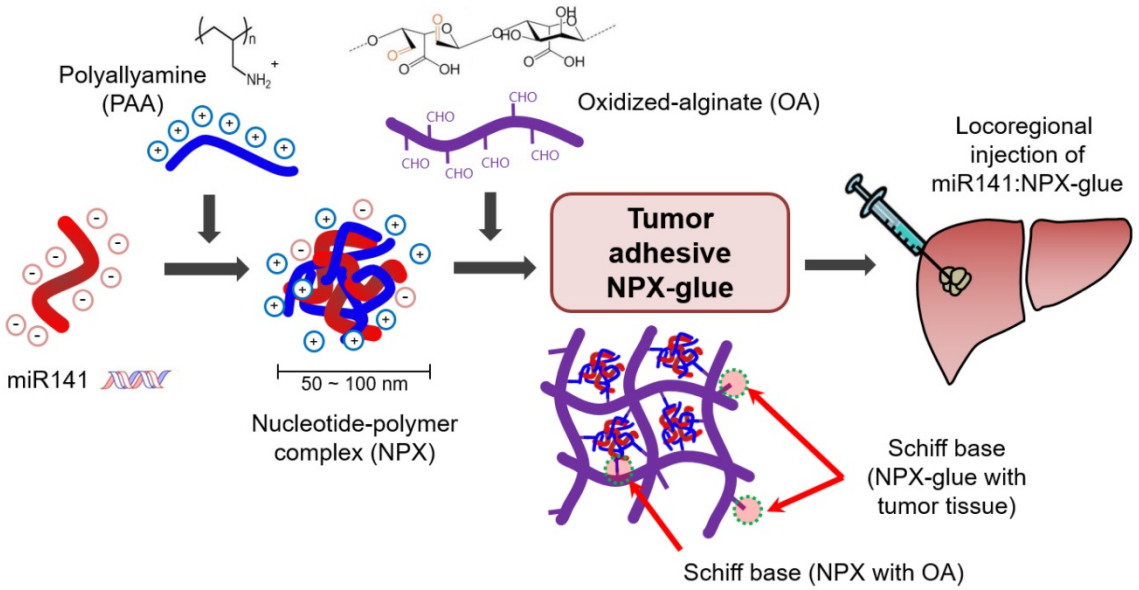

Scheme 1. Schiff base-forming tumor-adhesive hydrogel system (NPX-glue) for the locoregional tumor-suppressing gene (miR141) delivery to hepatic cellular carcinoma.

Methods

Materials

PAA (15%, average molecular weight 15 kDa) and sodium alginate (Protanal® LFR 5/60, high alpha-$_L$-guluronate (G) residues) were obtained from Polyscience Inc. (Warrington, PA, USA) and FMC Biopolymer (Sandvika, Norway), respectively. Diethylene glycol, sodium periodate, and dopamine hydrochloride were obtained from Sigma-Aldrich Inc. (St. Louis, MO, USA). Dulbecco's phosphate-buffered saline (DPBS), Dulbecco's modified Eagle's medium (DMEM), and 100× penicillin/streptomycin were obtained from Thermo Fisher Scientific (Waltham, MA, USA). Fetal bovine serum (FBS) was obtained from Hyclone (Pittsburgh, PA, USA) and 0.1% trypsin-EDTA was obtained from Welgene Inc. (Daegu, Korea). miR-141-5p mimic (5′-CAUCUUCCA GUACAGUGUUGGA-3′) and a negative control (NC) miRNA (5′-UUGUACUACACAAAAGUACUG-3′) were obtained from Genolution (Seoul, Korea). Plasmid pEGFP-C1 for the expression of the green fluorescent protein (GFP) was obtained from Clontech (Mountain View, CA, USA) and pLOC for the expression of the red fluorescent protein (RFP) was obtained from Thermo Scientific (Waltham, MA, USA).

Preparation of NPX and NPX-glue

NPX. All reagents for miRNAs were dissolved in diethylpyrocarbonate (DEPC)-treated water. The NPX contains PAA with miRNAs or plasmid DNA, which was prepared by a self-assembly process [35]. To generate NPX containing miRNA (miR:NPX), the 20-μM miRNA solution was mixed with a fixed volume of 15% PAA solution to obtain PAA/nucleic acid ratios (i.e., the ratio between amines (N) in PAA and phosphates (P) in miRNA; N/P ratios) from 0.03 to 32 (**Figure 1**). After a 30-min incubation at 4 °C, the miR:NPX was subjected to electrophoresis on a 2% agarose gel containing 50 μg/mL ethidium bromide in Tris-Acetate-EDTA (TAE) buffer. The agarose gel was illuminated under UV light to detect free miRNA. The sizes and the zeta potential of the NPX were measured using Philips CM200 T Transmission Electron Microscopy (TEM) and Zetasizer Nano-ZS90 (Malvern Instrument Ltd., Worcestershire, UK), respectively.

NPX-glue. Partially oxidized alginate (degree of aldehyde substitution in uronate: 30 mol%) was prepared by oxidation with sodium periodate. The detailed methods are described in Supplementary Material. The aldehyde content in oxidized alginate (OA) was measured using the hydroxylamine hydrochloride titration method [36, 37]. OA was added to NPX (2:1, v:v) and mixed to generate a gel, which was designated as NPX-glue (**Figure S1**).

In vitro serum stability assay for the miRNA in NPX

Four micrograms of miRNA alone or in NPX (N/P ratio of 16) was incubated in 10% FBS at 37 °C for the periods indicated in the figures. Sodium dodecyl sulfate (SDS) was added to the samples (final concentration was 1%, w/v) and mixed. The samples were subjected to electrophoresis on a 1.5% agarose gel, which was stained with ethidium bromide to visualize the miRNA band. The gel was analyzed by the Gel Documentation System (LSG-1000, iNtRON Biotechnology, Seongnam, Korea).

Determination of cytotoxicity of NPX and NPX-glue

Hep3B human hepatocellular carcinoma cells (ATCC HB-8064™) were purchased directly from ATCC at the beginning of the experiments and cultured in DMEM supplemented with 10% FBS, and 1× penicillin/streptomycin, and incubated at 37 °C under 5% CO_2. The cells were tested for Mycoplasma using the MicoProbe Mycoplasma Detection kit (R&D Systems, Minneapolis, MN, USA) and were confirmed to be negative for mycoplasma. Hep3B cells were plated at a density of 5×10^4 cells/well on a coverslip in a 24-well plate on day 0. On day 1, NPX or NPX-glue was added to the cells. In the case of NPX-glue, NPX-glue was placed on a side of the well and the coverslip containing the seeded cells was placed on the well. On day 3, the cells were trypsinized and the cell viabilities were determined using the Cell Counting Kit-8 (CCK-8; Dojindo Molecular Technologies, Inc, Rockville, MD, USA) as described in the manufacturer's protocol. The cell viability was determined by comparing the CCK-8 values for the treated cells with those of the untreated cells, which were regarded as 100% viable.

Determination of transfection efficiency of NPX-glue

NCmiR was labeled with Cy5 (^{Cy}5NCmiR) using LabelIT miRNA labeling kit (Mirus Bio, Madison, WI, USA). Thereafter, NPX containing Cy5NCmiR (^{Cy}5NCmiR:NPX-glue) or the pEGFP-C1 plasmid (pEGFP:NPX) were prepared as described above. To determine the transfection efficiency, Hep3B cells were plated at a density of 5×10^4 cells/well on a coverslip in a 24-well plate on day 0. On day 2, ^{Cy}5NCmiR:NPX-glue or pEGFP:NPX-glue was placed on a side of the well and the coverslip containing the seeded cells was placed on the well. On the days indicated in the figures, ^{Cy}5NCmiR or GFP expression

in the cells was determined using confocal fluorescence microscopy (Zeiss LSM510 Meta Confocal Imaging System, Carl Zeiss, Thornwood, NY, USA) and FACSCalibur Flow Cytometry (BD Biosciences, San Jose, CA, USA) after detaching the cells. The transfection efficiency of NPX-glue was compared with that of G-fectin (Genolution, Seoul, Korea) for miRNA and Lipofectamine 2000 (Invitrogen, Waltham, MA, USA) for the plasmid. The cells were transfected with ^{Cy5}NCmiR (100 nmol) or pEGFP-C1 (0.5 μg) using G-fectin or Lipofectamine 2000, respectively, as per the manufacturer's suggestion.

Total RNA isolation and quantitative real-time PCR (qPCR)

Total RNA was isolated from tissues or the transfected cells using the TRIzol reagent (Invitrogen, Waltham, MA, USA) according to the manufacturer's instructions. First strand cDNA was generated using a reverse transcription kit (Takara Bio Inc., Mountain View, CA, USA). The expressions of mature miRNAs and their target genes were measured as described previously [38]. Human *GAPDH* and *U6* were used to normalize the values within the different experimental groups. The nucleotide sequences of the primers used for the qPCR are presented in Supplementary Material. These experiments were repeated three times.

Application of NPX-glue in mice

Hep3B cells (5×10^6 cells) were injected into the subcutaneous tissue in a flank region of six-week-old male NOD.CB17-Prkdscid mice (Orient Bio, Korea). The size of the tumor was calculated as length × $(\text{width})^2$ × 0.5. To assess the delivery efficiency of NPX-glue *in vivo*, 100 μL of ^{Cy5}NCmiR:NPX-glue or pLOC:NPX-glue was injected into the tumors when the mean volume of the tumors reached approximately 100 mm^3. Fifty micrograms of ^{Cy5}NCmiR and 10 μg of pLOC for red fluorescent protein (RFP) expression were used in each group. The intensities of the Cy5 or the RFP were measured using an In-Vivo FX PRO Small-Animal Imaging System (Bruker, Billerica, MA, USA) under excitation and emission wavelengths of 558 nm and 583 nm, respectively, 3 and 30 days after injection. To assess the therapeutic effect of miRNA, NCmiR:NPX-glue or miR-141 was injected into the tumors. When the mean volume of the tumors reached approximately 250 mm^3, the mice were divided into two groups and injected with NCmiR:NPX-glue or miR-141:NPX-glue thrice every other day. The changes in tumor volume were monitored for 25 days. At the end of the experiments, the mice were euthanized, and the tumor tissues were harvested. All animal studies were approved by the Institutional Animal Care and Use Committee (IACUC) of Inha University.

Protein preparation and immunoblotting

Whole cell lysates were prepared from the harvested tissues or the cultured cells and immunoblotting was performed as described previously [17]. Twenty micrograms of the proteins was separated on a 10% SDS-PAGE and transferred onto a nitrocellulose membrane. Rabbit polyclonal antibody against MAP4K4 (mitogen-activated protein kinase kinase kinase kinase 4) was obtained from Abcam (Cambridge, MA, USA) and mouse monoclonal antibodies against TIAM1 (T-cell lymphoma invasion and metastasis), BCL-2 (apoptosis regulator), and β-actin were obtained from Santa Cruz Biotechnology (Dallas, TX, USA). Horseradish peroxidase-labeled goat anti-mouse and anti-rabbit IgG were obtained from Santa Cruz Biotechnology (Dallas, TX, USA) and used as the secondary antibodies.

TUNEL staining assay

TUNEL staining was performed using paraffin-embedded tumor tissues with the DeadEnd Fluorometric TUNEL System (Promega, Madison, WI, USA) as described previously [39]. Hematoxylin-Eosin was used for counterstaining.

Results

Formation and characterization of miRNA:NPX and miRNA:NPX-glue

Various kinds of cationic polymers have been used previously as delivery vehicles for nucleic acids [25–29]; we used PAA in this study. We formed complexes called NPX between PAA and either miRNA (miRNA:NPX) or plasmid DNA (plasmid:NPX). PAA and miR-141 were mixed in various ratios, which we called the N/P ratio, to determine the point where all the miR-141 was incorporated into NPX. The amount of free miR-141 was remarkably reduced as the N/P ratio increased from 0.03 to 0.8, and no visible free miR-141 was detected when the ratio was higher than 1.6 (**Figure 1A**), which was consistent with the zeta potentials of NPX (**Figure 1B**). The size of NPX determined by TEM was in the range of ~50–100 nm (**Figure 1C**). The stability of the miRNA in NPX was examined by incubating miR-141:NPX in serum. After the incubation, the amount of miRNA that remained in the complex was determined. Consistent with the zeta potential, miR-141 complexed with PAA in NPX in the reverse direction compared with free miR-141 and was stably detected even after 14 days, whereas all the

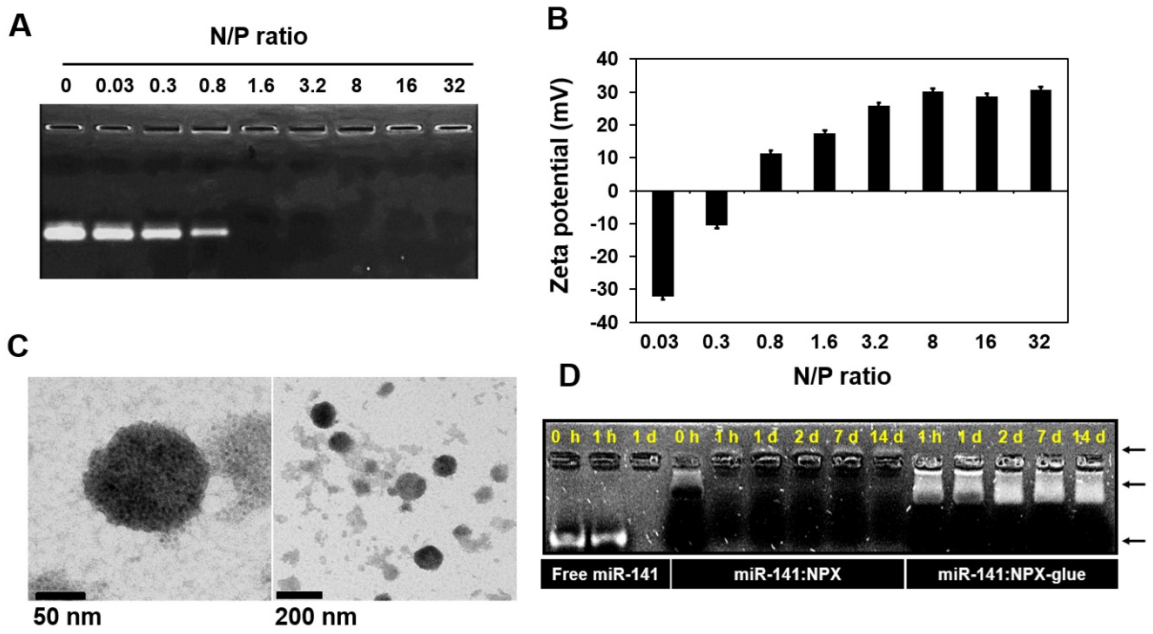

Figure 1. Formation of miR-141:NPX at various N/P ratios. (A) miR-141:NPX with the indicated N/P ratios were separated on an agarose gel. Free miR-141 not incorporated into the NPX is shown as bands. **(B)** miR-141:NPX with the indicated N/P ratios were prepared in PBS and diluted with deionized water. The zeta potentials of each NPX preparation was measured using Nano-ZS90 Malvern Zetasizer. The values are the mean ± standard deviation (S.D.) of three samples. **(C)** TEM images of NPX. One drop of the NPX solution with a N/P ratio of 1.0 was placed on a copper grid and negatively stained with 2% uranyl acetate. **(D)** Free miR-141, miR-141:NPX, or miR-141:NPX-glue with a N/P ratio of 1.6 was incubated with 10% FBS in PBS over the time indicated in the figure. At the end of the incubation, the samples were separated on an agarose gel. The remaining miR-141 can be seen as a band in the gel.

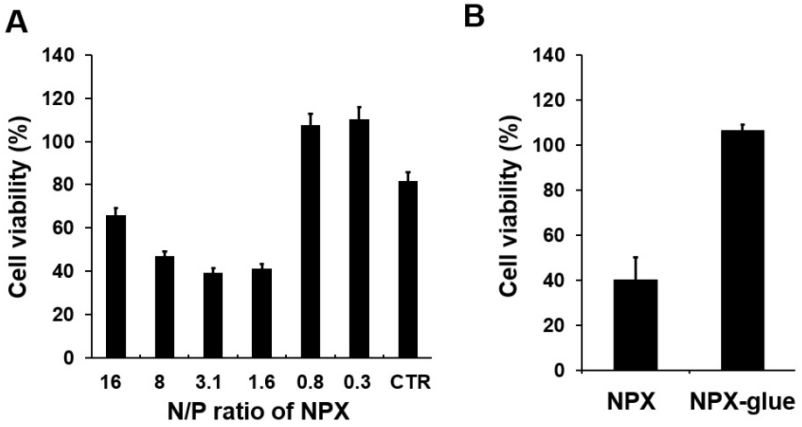

Figure 2. Cytotoxicity of NPX and NPX-glue with various N/P ratios. (A) Hep3B cells were plated at a density of 5×10^4 cells/well in 24-well plates on day 0. On day 1, the cells were treated with NCmiR:NPX with the indicated N/P ratios. The cell viability was determined on day 3. The cells transfected with Lipofectamine 2000 were the control (CTR) for this experiment. **(B)** Cells were treated with NCmiR:NPX (N/P ratio = 1.6) or NCmiR:NPX-glue (N/P ratio = 1.6) and their % cell viabilities were compared with that of the untreated cells, which were regarded as 100%. The values are mean ± S.D. calculated from three wells. * indicates a statistical significance of $p < 0.05$ using Student's *t*-test. The experiments were repeated three times.

free miR-141 was degraded and became undetectable within a day (**Figure 1D**).

We designed a Schiff base-forming tumor-adhesive hydrogel system by mixing NPX with OA, which was designated as NPX-glue. The tissue-adhesive property of NPX-glue is illustrated in **Figure S1A**. The mixture of NPX and OA quickly formed an injectable hydrogel (NPX-glue) that exhibited tissue-adhesive properties on an *in vitro* mucin disk and an *in vivo* tumor model (**Figure S1**). The complex of miR-141 and the NPX-glue (miR-141:NPX-glue) remained stable for 14 days before release. The miR-141 was located at a shifted position compared to the free form, which implies that miR-141 might be released to the buffer as NPX forms (**Figure 1D**).

NPX-glue is an efficient delivery molecule for nucleotides without cytotoxicity

Cytotoxicity of NPX and NPX-glue on Hep3B cells was examined using a non-specific negative control miRNA (NCmiRNA). When NPX with a N/P ratio higher than 1.6 was used, fewer than 50% of the cells were viable, while most of the cells incubated with the NPX with a N/P ratio lower than 0.8 were viable. (**Figure 2A** and **Figure S2**). However, when NCmiR:NPX-glue with a N/P ratio of 1.6 was added, most of the cells were viable (**Figure 2B**). These results

suggest that the NPX-glue formation with OA eliminated the inherent cytotoxic effect of NPX.

To evaluate how efficiently NPX-glue transfers miRNA to cells, the transfection efficiency of NPX-glue was compared with that of G-fectin, a transfection reagent for small RNA, using Cy5-labeled NCmiR (^{Cy5}NCmiR) in Hep3B cells. Hep3B cells were incubated with the blank NPX-glue, ^{Cy5}NCmiR:NPX-glue, or transfected with ^{Cy5}NCmiR using G-fectin. The cells emitting fluorescence due to the presence of ^{Cy5}NCmiR were counted 6 and 14 days after the treatment. A majority of the cells in the dish transfected with ^{Cy5}NCmiR using G-fectin emitted red fluorescence on day 1 and 6, but the fluorescence signal disappeared on day 14. However, approximately 45% of the cells exhibited fluorescence six days after the treatment with ^{Cy5}NCmiR:NPX-glue, which continued and approximately 57% of the cells emitted fluorescence on day 14 after the treatment (**Figure 3A-B**). The fluorescence mostly came from the cells around the ^{Cy5}NCmiR:NPX-glue boundary. NPX-glue also seemed to transfer plasmid DNA efficiently into cells. When pEGFP:NPX-glue was incubated with the cells, the cells around the glue boundary expressed GFP for 14 days. These results suggest that NPX-glue delivers ^{Cy5}NCmiR and plasmid into the cells. However, it should be noted that the fate of plasmids within the hydrogel is unlikely to be as reliably predicted as that of miRNA, given the significant difference in their sizes and thus their charge densities.

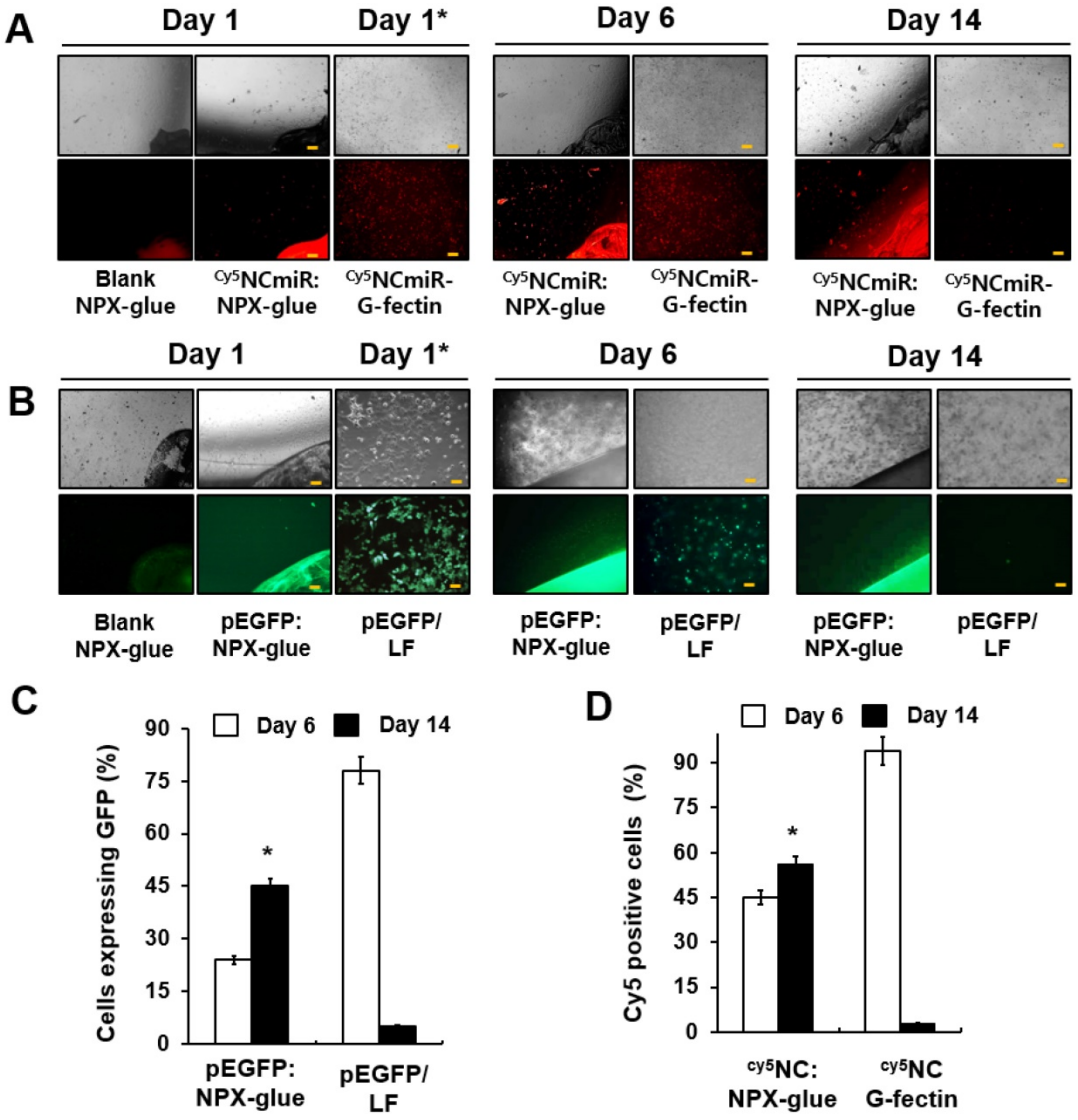

Figure 3. Gene delivery efficiency of NPX-glue into Hep3B cells. (A) Hep3B cells were plated on a coverslip in a 24-well plate on day 0. The blank NPX-glue or ^{Cy5}NCmiR:NPX-glue were placed on a side of the well under the culture media. The coverslips with the seeded Hep3B cells were placed in the well on day 1. Fluorescence from Cy5 was observed on days 6 and 14. Transfection of ^{Cy5}NCmiR using G-fectin was used as a control (^{Cy5}NCmiR-Gfectin) and the image was taken 24 h after transfection (Day 1*). **(B)** The blank NPX-glue or pEGFP:NPX-glue was placed on a side of the well under the culture media. The coverslips with the seeded Hep3B cells were placed in the well on day 1. The fluorescence from GFP was observed on days 6 and 14. Transfection of pEGFP using Lipofectamine 2000 was used as a control (pEGFP:LF) and the image was taken 24 h after transfection (Day 1*). 10X magnification (Scale bar) **(C)** Percentage of cells that expressed ^{Cy5}NCmiR on days 6 and 14. **(D)** Percentage of cells that expressed GFP on days 6 and 14. The values are the mean ± S.D. of three wells. The experiments were repeated three times.

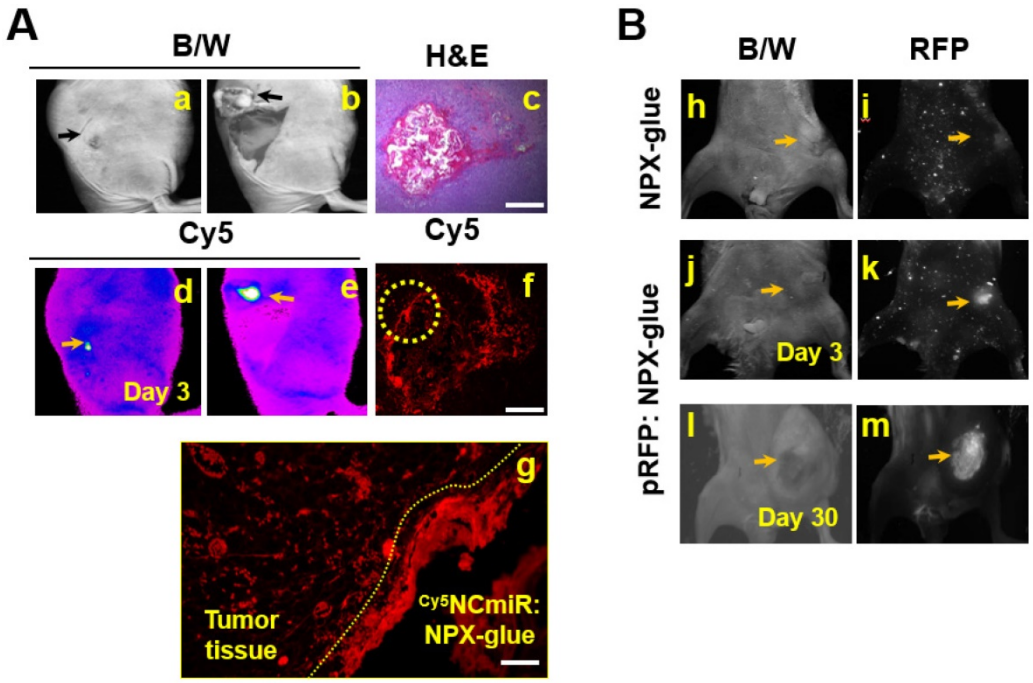

Figure 4. Gene delivery efficiency of NPX-glue *in vivo*. (A) ^{Cy5}NCmiR:NPX-glue was injected into a tumor implanted in mice. Three days after the injection, uptake of the miR into the tumor cells was observed. a. tumor region under bright white light (B/W) under the skin; b. tumor region under bright white light (B/W) with the skin removed; c. H&E staining of the tumor tissue injected with ^{Cy5}NCmiR:NPX-glue; d. e. tumor region covered with skin (d) or uncovered (e) taken by an In-Vivo FX PRO Small-Animal Imaging System; f. g. fluorescence microscopic observation of the tumor region at 4X (f) and 40X magnification (g). Yellow arrow indicates the tumor. The region marked with the yellow circle in (f) is magnified in (g). **(B)** The NPX-glue or pRFP:NPX-glue was injected into the tumors implanted in mice. On either the third or thirtieth day after injection, the tumor region was observed under bright white light (B/W) (h, j, l) or a fluorescence microscope (i, k, m). Yellow arrows indicate the tumor.

NPX-glue stably delivered nucleic acids to tumors *in vivo*

In order to determine if NPX-glue could deliver miRNA into the cells *in vivo*, ^{Cy5}NCmiR:NPX-glue was injected into an implanted hepatoma cell mass in mice and the fluorescence from ^{Cy5}NCmiR was measured three days after the injection (**Figure 4A**). We observed that the cells around the injected glue preferentially took up ^{Cy5}NCmiR. To make sure that the cells surrounding the glue took up and processed the nucleic acid, pRFP, a plasmid that expresses red fluorescent protein, was mixed with NPX-glue. pRFP:NPX-glue was injected into the implanted hepatoma cell mass in mice and the fluorescence from pRFP was measured 3 and 30 days after injection. Red fluorescence was detected from the tumor region 3 days after the injection, and continued to be detectable for up to 30 days (**Figure 4B**).

These results imply that NPX-glue can deliver miRNA and plasmid to a solid tumor efficiently *in vivo,* and allow long-term expression of the introduced gene. Thus, NPX-glue could be used with therapeutic nucleic acids.

miR-141:NPX-glue inhibited target gene expression

The regulatory effects of miR-141 on hepatic cancer cell proliferation, invasion, and migration have raised interest in the use of miR-141 as a therapeutic molecule for HCC [16, 22, 23]. The expression level of miR-141 is closely related to HCC progression and the overexpression of miR-141 in HCC significantly reduced cell proliferation and invasion [17, 23]. The effect of miR-141:NPX-glue on the miR-141 target genes was evaluated in Hep3B cells. Hep3B cells were cultured with miR-141:NPX-glue for 48 h and the introduction of miR-141 was confirmed by qPCR, which showed 150-fold more miR-141 in miR-141:NPX-glue-treated cells than in NCmiR:NPX-glue treated cells (**Figure 5A**). The mRNA level of other target genes of miR-141, such as *MAP4K4*, *TM4SF1* (transmembrane 4L six family member 1), *KEAP1* (Kelch-like ECH-associated protein 1), *HDGF* (heparin-binding growth factor), and *TIAM1*, were reduced by ~50–70% in the cells (**Figure 5B**). The blank NPX-glue did not result in a change of gene expression compared with untreated cells. These results suggest that miR-141 was delivered efficiently to the cells by miR-141:NPX-glue and successfully inhibited the target genes.

miR-141:NPX-glue inhibited tumor growth *in vivo*

The effects of miR-141:NPX-glue were evaluated in Hep3B cells (5×10^6 cells) injected subcutaneously in NOD.CB17-Prkdscid mice. When the size of the tumors reached 0.25×10^3 mm^3, miR-141:NPX-glue or NCmiR:NPX-glue was injected into the tumor, and

the growth of the tumors was monitored for 24 days. While the tumors injected with NCmiR:NPX-glue grew continuously and reached 2.5×10^3 mm^3 at the end of the study, the tumors injected with miR-141:NPX-glue grew to smaller sizes (**Figure 6A**). At the end of the observation, the size and weight of the tumors injected with miR-141:NPX-glue were approximately 50% of those injected with NCmiR:NPX-glue (**Figure 6B**). The body weight of the mice injected with NPX-glue, either with NCmiR or miR-141, did not change during the experiment, which suggests that NPX-glue may be a nontoxic molecule for the animals (**Figure 6C**). The tumor tissues around the injection site of miR-141:NPX-glue underwent apoptosis, which was determined by TUNEL staining (**Figure 6D**). The tumor tissues were collected and the target proteins of miR-141 and the proteins involved in apoptosis and anti-apoptosis were analyzed. In the tissues injected with miR-141:NPX-glue, the expression of MAP4K4 and TIAM1, the target proteins of miR-141, were reduced. The expression of BCL-2, an anti-apoptotic protein, decreased while the expression of cleaved caspase 3, an apoptotic protein, increased in the tissues injected with miR-141:NPX-glue (**Figure 6E**), as compared with tissues injected with NCmiR:NPX-glue. This suggests that miR-141:NPX-glue successfully delivered miR-141 to the tumor tissue, where it inhibited the target genes and induced apoptosis, resulting in the suppression of tumor growth.

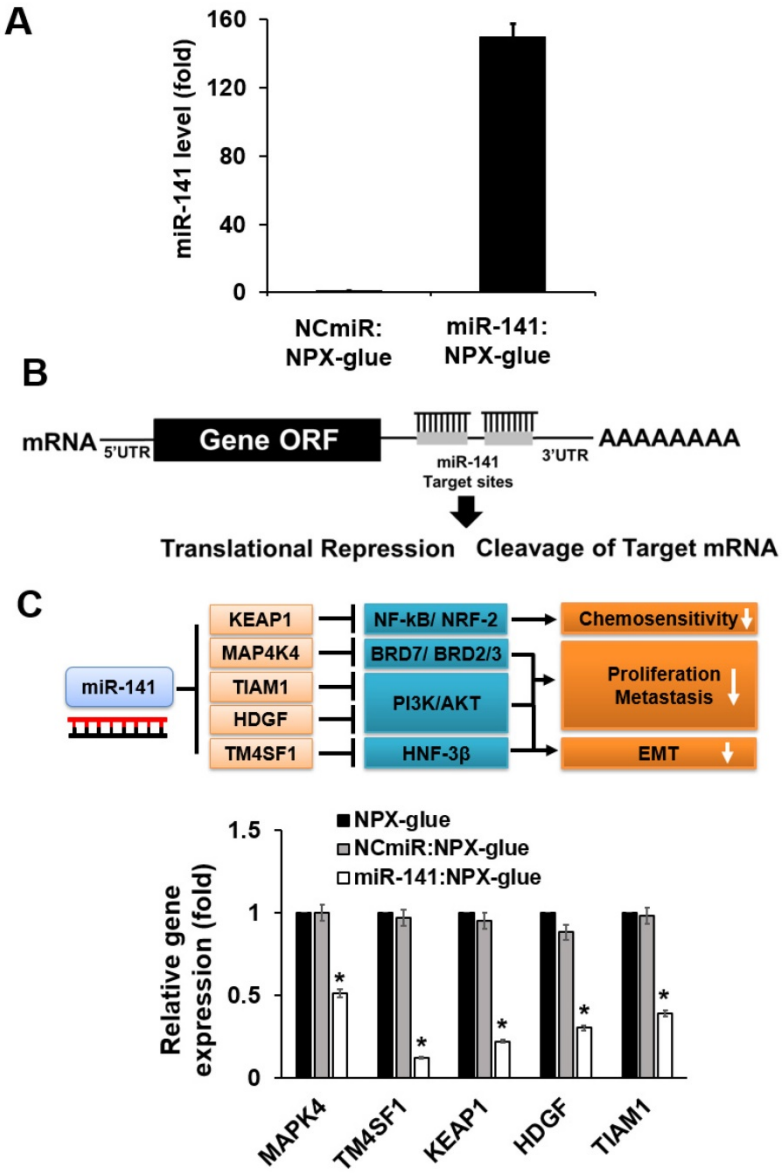

Figure 5. Expression levels of the target genes in the cells treated with miR-141:NPX-glue. (A) Cellular expression level of miR-141 when Blank NPX-glue, NCmiR:NPX-glue, or miR-141:NPX-glue was placed on the side of the well in a 6-well plate. Coverslips seeded with Hep3B cells were placed into the wells on day 1. On day 3, the cells were harvested, total RNA was extracted from the cells, and qPCR was performed to measure the expression level of miR-141. **(B)** Schematic drawing of inhibition of the target genes by miR-141. **(C)** The mRNA expression levels of *MAP4K4*, *TM4SF1*, *KEAP1*, *HDGF*, and *TIAM1*. The mRNA expression levels were normalized against GAPDH and the relative expression levels of each mRNA were compared with those of blank NPX-glue-treated cells. The values are the mean ± S.D. of three wells. * indicates a statistical significance of $p < 0.05$ using Student's *t*-test. The experiments were repeated three times.

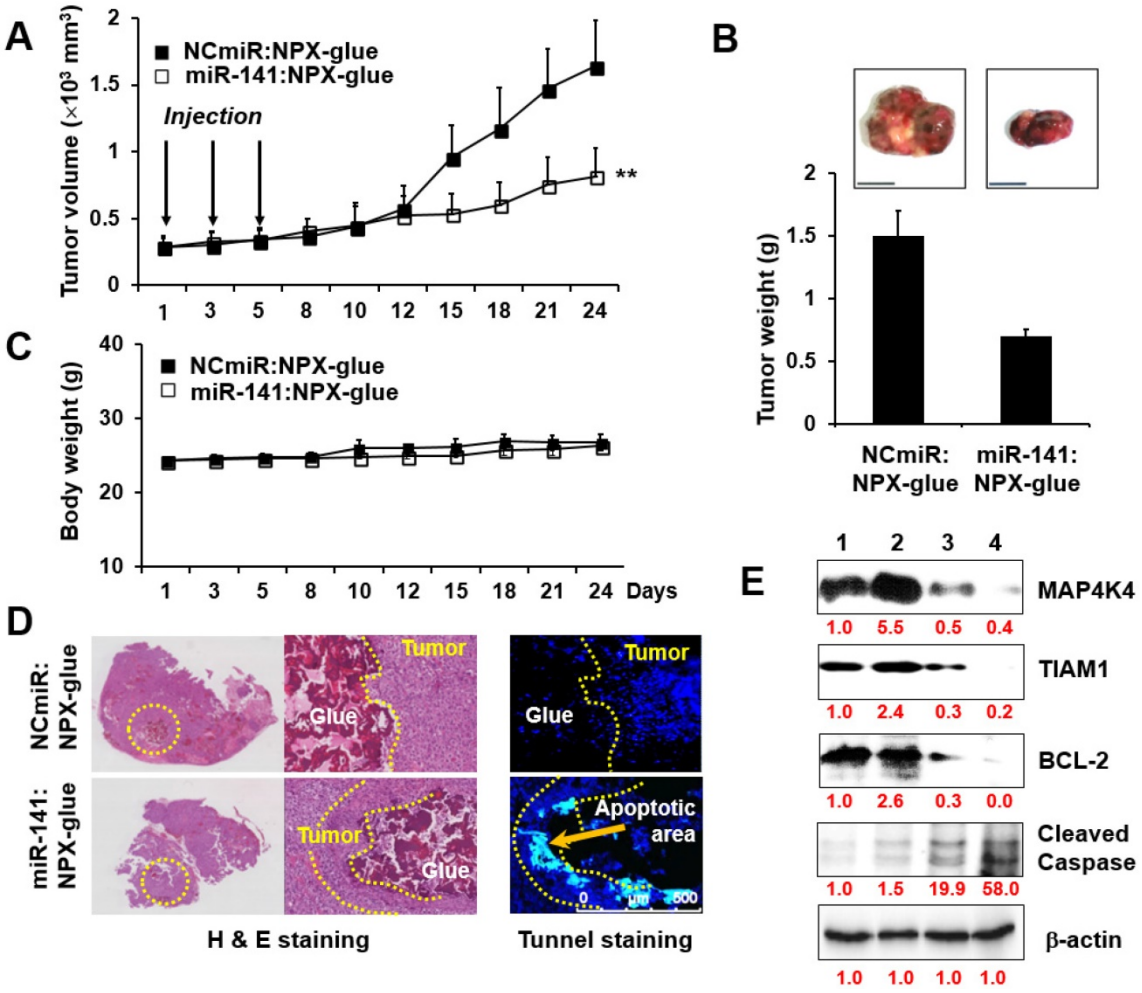

Figure 6. Tumor-suppressive effect of miR-141:NPX-glue. (A) Hep3B cells (5×10^4 cells) were injected subcutaneously (SQ) into the flank of mice. When the tumor size reached 250 mm³, NCmiR:NPX-glue or miR-141:NPX-glue was injected into the tumors thrice. The volumes of the tumors were monitored for 24 days. **(B)** The tumors were harvested 24 days after injection and their weight was measured. The values are the mean ± S.D. of three tumors. **(C)** Body weights of the mice were monitored during the experiment. The values are the mean ± S.D. of five mice. **(D)** H&E and TUNEL staining of the tumor tissues treated with NCmiR:NPX-glue or miR-41:NPX-glue. The yellow arrow indicates apoptotic area. **(E)** Immunoblot analysis of MAP4K4, TIAM1, BCL-2, cleaved caspase 3, and β-actin in the tissues treated with NCmiR:NPX-glue (lanes 1 and 2) and miR-141:NPX-glue (lanes 3 and 4). Values of the band intensity (in red characters) measured by Image J are shown below the figures. ** indicates a statistical significance of $p < 0.05$ using Student's *t*-test. The experiments were repeated three times.

Discussion

In this study, we developed a novel system that enables the local delivery of nucleic acids to a solid tumor and investigated its effectiveness in mice. PAA, a cationic polymer, was used as the delivery vehicle for the nucleic acids, both miRNA and plasmid DNA. The PAA-nucleic acid complex (NPX) itself was an efficient gene delivery molecule in cultured cells [31, 33, 34]. The ionic complex of PAA and nucleic acids was mixed with OA and transformed into a tissue-adhesive hydrogel, the NPX-glue, which secured the delivery of nucleic acids in tissues. More specifically, cationic PAA containing amines formed nano-sized ionic complexes (NPX) with anionic nucleic acids (miR-141 or plasmids), and then the residual amines of NPX reacted with aldehydes of OA to form a stable hydrogel. This NPX-loaded hydrogel acted as a tissue-adhesive glue after intratumoral injection owing to the additional Schiff base formation between the aldehydes of OA and tissue proteins. The associated nucleic acid was released from this complex and entered cells. When miR-141 was the nucleic acid incorporated, it exhibited tumor-suppressing effects over an extended period.

NPX was cytotoxic when the N/P ratio was over 0.8, but the formation of NPX-glue virtually eliminated the cytotoxic effects. The Schiff base formation between the amines of PAA and the aldehydes of OA could be responsible for attenuating the toxicity of NPX (**Figure 2B**). The benefits of the NPX-glue that we developed include: 1) NPX-glue formation is a simple and fast self-cross-linking process that is induced by a simple blending of OA and PAA solutions; 2) the NPX-glue quickly and securely adheres to tissues after injection; 3) the NPX-glue locally releases therapeutic nucleotides including miRNA for extended periods with stability; and 4) it is biodegradable [24, 25].

Various nucleotides can be delivered by NPX-glue. In this study, short RNA molecules like miR-141 were delivered *in vivo* by NPX-glue and successfully inhibited the target genes in the surrounding tissues. We also showed that long plasmid DNA that encoded RFP expressed RFP *in vivo* upon delivery by NPX-glue. These results suggest that NPX-glue could be used as a delivery molecule for a wide range of gene therapies.

miR-141 has been suggested to have tumor suppressive effects [17, 23]. We introduced miR-141 in the form of NPX-glue and examined the efficiency of gene delivery and the tumor suppressive effects of miR-141 in HCC cells implanted in mice. The NPX-glue in the tumor successfully delivered miR-141 to the region of injection and the surrounding tissues, and effectively inhibited target genes such as *MAP4K4*, *TM4SF1*, *KEAP1*, *HDGF*, and *TIAM1*. The inhibition of miR-141 target genes resulted in apoptosis and tumor growth suppression. We cannot infer the exact molecular mechanism by which miR-141 induced apoptosis, but it was probably through its combined effects on various genes. The results suggest that NPX-glue associated with a tumor suppressor is an excellent therapeutic strategy, especially for tumors that need size reduction before further treatment. It may also be applied directly to surgical sites after resection of a tumor as a postoperative treatment to kill residual tumor cells and prevent tumor metastasis. Moreover, the expression of GFP shown in the surrounding tissues from pEGFP:NPX-glue injection also suggests the possibility of combining several genes or long plasmids with miRNAs. Indeed, the overexpression of a tumor suppressor gene and the introduction of tumor suppressor miRNA could be combined for better results. Although the NPX-glue system was effective for the implanted HCC in this study, studies involving endogenous HCC will be necessary.

In conclusion, we developed a tissue-adhesive NPX-glue that can deliver nucleic acids efficiently and safely to tissues. When miR-141, a tumor suppressive miRNA, was used as a therapeutic molecule in the form of NPX-glue and injected into an implanted HCC, miR-141 was delivered to the surrounding tumor tissues and successfully inhibited tumor growth. Therefore, NPX-glue can be a useful locoregional therapeutic molecule to deliver nucleic acids safely and effectively for an extended period.

Abbreviations

GFP: green fluorescent protein; HCC: hepatocellular carcinoma; NC: negative control; NPX: nanocomplex; OA: oxidized alginate; PAA: polyallylamine; RFP: red fluorescent protein; SDS: sodium dodecyl sulfate.

Acknowledgements

This research was supported by Basic Science Research Program and Korea Research Fellowship Program through the National Research Foundation of Korea (NRF) (2017R1A2A2A07001272, 2017R1A6A3A11035722, 2016H1D3A1938159, and 2015R1D1A1A01059023 and 2018R1A6A1A03025523) and partly supported by WCSL (World Class Smart Lab) research grant directed by Inha University.

Supplementary Material

Supplementary methods, figures and table.
http://www.thno.org/v08p3891s1.pdf

Competing Interests

The authors have declared that no competing interest exists.

References

1. Park J-W, Chen M, Colombo M, Roberts LR, Schwartz M, Chen P-J, et al. Global patterns of hepatocellular carcinoma management from diagnosis to death: the BRIDGE Study. Liver Int. 2015; 35: 2155-66.
2. Poon RT, Fan ST, Tsang FH, Wong J. Locoregional therapies for hepatocellular carcinoma: a critical review from the surgeon's perspective. Ann Surg. 2002; 235: 466-86.
3. Gbolahan OB, Schacht MA, Beckley EW, LaRoche TP, O'Neil BH, Pyko M. Locoregional and systemic therapy for hepatocellular carcinoma. J Gastrointest Oncol. 2017; 8: 215-28.
4. Hong K, Georgiades CS, Geschwind JF. Technology insight: image-guided therapies for hepatocellular carcinoma intra-arterial and ablative techniques. Nat Clin Pract Oncol. 2006; 3: 315-24.
5. Lencioni R, Crocetti L. Image-guided thermal ablation of hepatocellular carcinoma. Crit Rev Oncol Hematol. 2008; 66: 200-7.
6. Lencioni R. Locoregional treatment of hepatocellular carcinoma. Hepatology. 2010; 52: 762-73.
7. El-Serag HB. Hepatocellular carcinoma. N Engl J Med. 2011; 365: 1118-27.
8. Crissien AM, Frenette C. Current management of hepatocellular carcinoma. Gastroenterol Hepatol (NY). 2014; 10: 153-61.
9. Kitai S, Kudo M, Nishida N, Izumi N, Sakamoto M, Matsuyama Y, et al. Survival benefit of locoregional treatment for hepatocellular carcinoma with advanced liver cirrhosis. Liver Cancer. 2016; 5: 175-89.
10. Spadi R, Brusa F, Ponzetti A, Chiappino I, Birocco N, Ciuffreda L, et al. Current therapeutic strategies for advanced pancreatic cancer: A review for clinicians. World J Clin Oncol. 2016; 7: 27-43.
11. Löppenberg B, Sood A, Dalela D, Karabon P, Sammon JD, Vetterlein MW, et al. Variation in locoregional prostate cancer care and treatment trends at commission on cancer designated facilities: A National Cancer Data Base Analysis 2004 to 2013. Clin Genitourin Cancer. 2017; 15: e955-68.
12. Moran MS. Radiation therapy in the locoregional treatment of triple-negative breast cancer. Lancet Oncol. 2015; 16: e113-e22.
13. Poon RT, Fan ST, Lo CM, Liu CL, Wong J. Long-term survival and pattern of recurrence after resection of small hepatocellular carcinoma in patients with preserved liver function: implications for a strategy of salvage transplantation. Ann Surg. 2002; 235: 373-82.
14. Lin DY, Lin SM, Liaw YF. Nonsurgical treatment of hepatocellular carcinoma. J Gastroenterol Hepatol. 1997; 12: S319-S28.
15. Bartel DP. MicroRNAs: genomics, biogenesis, mechanism, and function. Cell. 2004; 116: 281-97.
16. Kong YW, Ferland-McCollough D, Jackson TJ, Bushell M. MicroRNAs in cancer management. Lancet Oncol. 2012; 13: e249-e58.
17. Liu Y, Ding Y, Huang J, Wang S, Ni W, Guan J, et al. MiR-141 suppresses the migration and invasion of HCC cells by targeting Tiam1. PLoS One. 2014; 9: e88393.
18. Nakada C, Matsuura K, Tsukamoto Y, Tanigawa M, Yoshimoto T, Narimatsu T, et al. Genome wide microRNA expression profiling in renal cell carcinoma: significant down regulation of miR-141 and miR-200c. J Pathol. 2008; 216: 418-27.

19. Shimono Y, Zabala M, Cho RW, Lobo N, Dalerba P, Qian D, et al. Downregulation of miRNA-200c links breast cancer stem cells with normal stem cells. Cell. 2009; 138: 592-603.
20. Xu L, Li Q, Xu D, Wang Q, An Y, Du Q, et al. Hsa-miR-141 downregulates TM4SF1 to inhibit pancreatic cancer cell invasion and migration. Int J Oncol. 2014; 44: 459-66.
21. Du Y, Xu Y, Ding L, Yao H, Yu H, Zhou T, et al. Down-regulation of miR-141 in gastric cancer and its involvement in cell growth. J Gastroenterol. 2009; 44: 556-61.
22. Jiang J, Gusev Y, Aderca I, Mettler TA, Nagorney DM, Brackett DJ, et al. Association of microRNA expression in hepatocellular carcinomas with hepatitis infection, cirrhosis, and patient survival. Clin Cancer Res. 2008; 14: 419-27.
23. Lin L, Liang H, Wang Y, Yin X, Hu Y, Huang J, et al. microRNA-141 inhibits cell proliferation and invasion and promotes apoptosis by targeting hepatocyte nuclear factor-3β in hepatocellular carcinoma cells. BMC Cancer. 2014; 14: 879.
24. Gao C, Liu M, Chen J, Zhang X. Preparation and controlled degradation of oxidized sodium alginate hydrogel. Polym Degrad Stab. 2009; 94: 1405-10.
25. Boontheekul T, Kong H-J, Mooney DJ. Controlling alginate gel degradation utilizing partial oxidation and bimodal molecular weight distribution. Biomaterials. 2005; 26: 2455-65.
26. Sun J, Tan H. Alginate-based biomaterials for regenerative medicine applications. Materials. 2013; 6: 1285-309.
27. Liu Z, Jiao Y, Wang Y, Zhou C, Zhang Z. Polysaccharides-based nanoparticles as drug delivery systems. Adv Drug Deliv Rev. 2008; 60: 1650-62.
28. Artzi N, Shazly T, Baker AB, Bon A, Edelman ER. Aldehyde-amine chemistry enables modulated biosealants with tissue-specific adhesion. Adv Mater. 2009; 21: 3399-403.
29. Jeon O, Samorezov JE, Alsberg E. Single and dual crosslinked oxidized methacrylated alginate/PEG hydrogels for bioadhesive applications. Acta Biomater. 2014; 10: 47-55.
30. Lv H, Zhang S, Wang B, Cui S, Yan J. Toxicity of cationic lipids and cationic polymers in gene delivery. J Control Release. 2006; 114: 100-9.
31. Guo J, O'Mahony AM, Cheng WP, O'Driscoll CM. Amphiphilic polyallylamine based polymeric micelles for siRNA delivery to the gastrointestinal tract: In vitro investigations. Int J Pharm. 2013; 447: 150-7.
32. Höbel S, Aigner A. Polyethylenimines for siRNA and miRNA delivery in vivo. Wiley Interdiscip Rev Nanomed Nanobiotechnol. 2013; 5: 484-501.
33. Oskuee RK, Dosti F, Gholami L, Malaekeh-Nikouei B. A simple approach for producing highly efficient DNA carriers with reduced toxicity based on modified polyallylamine. Mater Sci Eng C Mater Biol Appl. 2015; 49: 290-6.
34. Wytrwal M, Leduc C, Sarna M, Goncalves C, Kepczynski M, Midoux P, et al. Gene delivery efficiency and intracellular trafficking of novel poly(allylamine) derivatives. Int J Pharm. 2015; 478: 372-82.
35. Wan Y-L, Zheng S-S, Zhao Z-C, Li M-W, Jia C-K, Zhang H. Expression of co-stimulator 4-1BB molecule in hepatocellular carcinoma and adjacent non-tumor liver tissue, and its possible role in tumor immunity. World J Gastroenterol. 2004; 10: 195-9.
36. Rutz S, Scheffold A. Towards in vivo application of RNA interference-new toys, old problems. Arthritis Res Ther. 2004; 6: 78-85.
37. Pardridge WM. Intravenous, non-viral RNAi gene therapy of brain cancer. Expert Opin Biol Ther. 2004; 4: 1103-13.
38. Balcells I, Cirera S, Busk PK. Specific and sensitive quantitative RT-PCR of miRNAs with DNA primers. BMC Biotechnol. 2011; 11: 70.
39. De la Rosa ÁJ, Rodríguez-Hernández Á, González R, Romero-Brufau S, Navarro-Villarán E, Barrera-Pulido L, et al. Antitumoral gene-based strategy involving nitric oxide synthase type III overexpression in hepatocellular carcinoma. Gene Ther. 2016; 23: 67-77.